Optical coherence tomography of cell dynamics in three-dimensional tissue models

Wei Tan, Amy L. Oldenburg

Biophotonics Imaging Laboratory
Beckman Institute for Advanced Science and Technology
Department of Electrical and Computer Engineering
University of Illinois at Urbana-Champaign

James J. Norman, Tejal A. Desai

Department of Biomedical Engineering
Boston University

Stephen A. Boppart

Biophotonics Imaging Laboratory
Beckman Institute for Advanced Science and Technology
Department of Electrical and Computer Engineering,
Department of Bioengineering, Department of Internal Medicine
University of Illinois at Urbana-Champaign
405 N. Mathews Avenue, Urbana, IL 61801
boppart@uiuc.edu

Abstract: Three-dimensional cell-based tissue models have been increasingly useful in the fields of tissue engineering, drug discovery, and cell biology. While techniques for building these tissue models have been advanced, there have been increasing demands for imaging techniques that are capable of assessing complex dynamic three-dimensional cell behavior in real-time and at larger depths in highly-scattering scaffolds. Understanding these cell behaviors requires advanced imaging tools to progress from characterizing two-dimensional cell cultures to complex, highly-scattering, thick three-dimensional tissue constructs. Optical coherence tomography (OCT) is an emerging biomedical imaging technique that can perform cellular-resolution imaging *in situ* and in real-time. In this study, we demonstrate that it is possible to use OCT to evaluate dynamic cell behavior and function in a quantitative fashion in four dimensions (three-dimensional space plus time). We investigated and characterized in thick tissue models a variety of cell processes, such as chemotaxis migration, proliferation, de-adhesion, and cell-material interactions. This optical imaging technique was developed and utilized in order to gain new insights into how chemical and/or mechanical microenvironments influence cellular dynamics in multiple dimensions. With deep imaging penetration and increased spatial and temporal resolution in three-dimensional space, OCT will be a useful tool for improving our understanding of complex biological interactions at the cellular level.

OCIS codes: (170.4500) Optical coherence tomography; (170.6900) Three-dimensional microscopy; (170.5380) Physiology; (170.1530) Cell analysis

References and links

1. R. Langer and J. P. Vacanti, "Tissue engineering," Science **260**, 920-926 (1993).
2. M. J. Friedrich, "Studying cancer in three dimensions: 3-D models foster new insights into tumorigenesis," JAMA **290**, 1977-1979 (2003).

#71557 - $15.00 USD Received 31 May 2006; revised 19 July 2006; accepted 20 July 2006

3. D. J. Stephens and V. J. Allan, "Light microscopy techniques for live cell imaging," Science **300**, 82-86 (2003).
4. R. G. M. Breuls, A. Mol, R. Petterson, C. W. J. Oomens, F. P. T. Baaijens, and C. V. C. Bouten, "Monitoring local cell viability in engineered tissues: A fast, quantitative, and nondestructive approach," Tissue Eng. **9**, 269-281 (2003).
5. D. S. Gareau, P. R. Bargo, W. A. Horton, and S. L. Jacques, "Confocal fluorescence spectroscopy of subcutaneous cartilage expressing green fluorescent protein versus cutaneous collagen autofluorescence," J. Biomed. Opt. **9**, 254-258 (2004).
6. B. R. Masters, P. T. So, and E. Gratton, "Multiphoton excitation microscopy of *in vivo* human skin. Functional and morphological optical biopsy based on three-dimensional imaging, lifetime measurements and fluorescence spectroscopy," Ann. N. Y. Acad. Sci. **838**, 58-67 (1998).
7. P. T. So, C. Y. Dong, B. R. Masters, and K. M. Berland, "Two-photon excitation fluorescence microscopy," Ann. Rev. Biomed. Eng. **2**, 399-429 (2000).
8. I. Constantinidis, C. L. Stabler, R. Long, and A. Sambanis, "Noninvasive monitoring of a retrievable bioartificial pancreas *in vivo*," Ann. N. Y. Acad. Sci. **961**, 298-301 (2002).
9. A. S. P. Lin, T. H. Barrows, S. H. Cartmella, and R. E. Guldberg, "Microarchitectural and mechanical characterization of oriented porous polymer scaffolds," Biomaterials **24**, 481-489 (2003).
10. D. Huang, E. A. Swanson, C. P. Lin, J. S. Schuman, W. G. Stinson, W. Chang, M. R. Hee, T. Flotte, K. Gregory, C. A. Puliafito, and J. G. Fujimoto, "Optical coherence tomography," Science **254**, 1178-1181 (1991).
11. B. E. Bouma and G. J. Tearney, editors, *Handbook of Optical Coherence Tomography*. Marcel Dekker, N.Y. (2001).
12. J. M. Schmitt, "Optical coherence tomography (OCT): a review," IEEE J. Select. Topics. Quantum Electon. **5**, 1205-1215 (1999).
13. J. G. Fujimoto, "Optical coherence tomography for ultrahigh resolution *in vivo* imaging," Nat. Biotechnol. **21**, 1361-1367 (2003).
14. S. A. Boppart, B. E. Bouma, C. Pitris, J. F. Southern, M. E. Brezinski, and J. G. Fujimoto, "*In vivo* cellular optical coherence tomography imaging," Nat. Med. **4**, 861-865 (1998).
15. A. G. Podoleanu, J. A. Rogers, D. A. Jackson, and S. Dunne, "Three dimensional OCT images from retina and skin," Opt. Express **7**, 292-298 (2000).
16. S. A. Boppart, M. E. Brezinski, B. E. Bouma, G. J. Tearney, and J. G. Fujimoto, "Investigation of developing embryonic morphology using optical coherence tomography," Dev. Biol. **177**, 54-63 (1996).
17. S. A. Boppart, G. J. Tearney, B. E. Bouma, J. F. Southern, M. E. Brezinski, and J. G. Fujimoto, "Noninvasive assessment of the developing *Xenopus* cardiovascular system using optical coherence tomography," Proc. Natl. Acad. Sci. USA **94**, 4256-4261 (1997).
18. X. Xu, R. K. Wang, and A. El Haj, "Investigation of changes in optical attenuation of bone and neuronal cells in organ culture or three-dimensional constructs *in vitro* with optical coherence tomography: relevance to cytochrome oxidase monitoring," Eur. Biophys. J. **32**, 355-362 (2003).
19. C. Mason, J. F. Markusen, M. A. Town, P. Dunnill, and R. K. Wang, "The potential of optical coherence tomography in the engineering of living tissue," Phys. Med. Biol. **49**, 1097-1115 (2004).
20. H. Michna, "Induced locomotion of human and murine macrophages: a comparative analysis by means of the modified Boyden-chamber system and the agarose migration assay," Cell Tissue Res. **255**, 423-429 (1989).
21. D. L. Marks, A. L. Oldenburg, J. J. Reynolds, and S. A. Boppart, "Study of an ultrahigh-numerical-aperture fiber continuum generation source for optical coherence tomography," Opt. Lett. **27**, 2010-2012 (2002).
22. T. S. Ralston, D. L. Marks, P. S. Carney, and S. A. Boppart, "Inverse scattering for optical coherence tomography," J. Opt. Soc. Am. A **23**, 1027-1037 (2006).
23. H. Steller, "Mechanisms and genes of cellular suicide," Science **267**, 1445-1449 (1995).
24. P. A. DiMilla, J. A. Quinn, S. M. Albelda, and D. A. Lauffenburger, "Measurement of individual cell migration parameters for human tissue cells," Amer. Inst. Chem. Engr. J. **38**, 1092-1104 (1992).
25. E. Cukierman, R. Pankov, D. R. Stevens, and K. M. Yamada, "Taking cell-matrix adhesions to the third dimension," Science **294**, 1708-1712 (2001).
26. N. L'Heureux, S. Paquet, R. Labbe, L. Germain, and F. A. Auger. "A completely biological tissue-engineered human blood vessel," FASEB J. **12**, 47-56 (1998).
27. H. W. Ouyang, S. L. Toh, J. Goh, T. E. Tay, and K. Moe, "Assembly of bone marrow stromal cell sheets with knitted poly (L-Lactide) scaffold for engineering ligament analogs," J. Biomed. Mat. Res. **75**, 264-271 (2005).
28. W. Tan, A. Sendmir-Urkmez, L. J. Fahrner, R. Jamison, D. Leckband, and S. A. Boppart, "Structural and functional optical imaging of three-dimensional engineered tissue development," Tissue Eng. **10**, 1747-1756 (2004).

#71557 - $15.00 USD Received 31 May 2006; revised 19 July 2006; accepted 20 July 2006

1. Introduction

Cell activities in three-dimensional (3-D) tissue models are of great interest for both basic cell biology research and applications, such as tissue engineering and pharmacological research [1,2]. Invasive imaging methods such as histology and scanning electron microscopy are used predominantly to evaluate cell activities and cellular responses to environmental stimuli in tissue models. These destructive methods, however, have intrinsic disadvantages. These methods do not permit real-time or dynamic imaging, lack real 3-D information, require long and harsh processing steps at discrete time points, and make structure–function correlations difficult. Consequently, despite tremendous increasing interest in this area, few have investigated the dynamics of cell behaviors in tissue models. The primary limitation has been inadequate imaging technology for high-resolution, real-time, noninvasive imaging deep within highly-scattering tissues.

Confocal microscopy has been an important advance in microscopy and has enabled the imaging of intact, optically nontransparent specimens to produce high-resolution (submicron) images of tissue structure with the use of fluorescent probes [3-5]. For a relatively thick specimen, confocal microscopy accomplishes optical sectioning by scanning the specimen with a focused beam of light and collecting the fluorescence signal via a pinhole aperture that spatially rejects light from out-of-focus areas of the specimen. Imaging depths, however, are limited to approximately one-hundred microns and exogenous fluorescence probes are usually required for detection, often limiting the long-term viability of the cells being imaged. Multiphoton microscopy, which relies on the simultaneous absorption of two or more near-infrared photons from a high-intensity short-pulse laser (most commonly a mode-locked titanium:sapphire laser) extends the imaging depth of confocal, but still with depth limitations of about 400–500 μm [6,7]. Newer technologies for imaging tissue models, including high-field-strength magnetic resonance imaging and microcomputed tomography, have been pursued for the assessment of cell and scaffold structure, with limited success. These techniques, with long data acquisition rates, hazards associated with high-energy radiation, and relatively high costs, are less suitable for both real-time and long-term imaging [8,9].

Optical coherence tomography (OCT) is an emerging technique that has the potential for overcoming many of the limitations of the current technologies [10, 11]. OCT combines the high resolutions of most optical techniques with an ability to reject multiply-scattered photons and, hence, image at cellular resolutions (several microns) up to several millimeters deep in nontransparent (highly-scattering) tissue. Because OCT relies on variations in refractive index which results in optical scattering for image contrast, no exogenous fluorophores are necessary, enabling cellular imaging within living specimens over time without loss of viability. Because longer wavelength near-infrared light is scattered less than visible light, it enhances visualization of changes at greater depths. OCT has been applied *in vivo* for imaging the microstructures of different tissues including the eye, skin, gastrointestinal tracts, and neural systems, to name only a few, and is becoming a promising and powerful imaging technology that has widespread applications throughout many fields of medicine and biology [12-17]. However, few studies have investigated the use of the OCT technology for monitoring cell dynamics in tissue models for tissue engineering [18, 19].

In this article, we report the use of OCT as a noninvasive imaging modality to explore 3-D cell activities in tissue models. OCT is capable of clearly identifying cells, and determining their position, distribution, and general morphology in 3-D. For the first time, we investigate and characterize cell dynamics and processes including chemotaxis migration, proliferation, de-adhesion, and cell-material interactions. This optical imaging technique was developed and utilized in order to gain new insights into how chemical microenvironments influence cellular functions and dynamics in multi-dimensional models. Compared to other microscopy approaches, OCT permits high-resolution, real-time, deep-tissue, 3-D imaging to be performed rapidly and repeatedly over extended periods of time with intact, living tissue models, with the potential to extend imaging of scaffolds to *in vivo* applications, such as following grafting of engineered tissues into a host tissue.

#71557 - $15.00 USD Received 31 May 2006; revised 19 July 2006; accepted 20 July 2006

2. Materials and methods

2.1 Cell and engineered tissue cultures

Tissue models are composed of cells, matrix scaffolds, or synthetic polymer scaffolds. In this study, NIH 3T3 fibroblast cells (American Type Culture Collection [ATCC], Manassas, VA), green-fluorescent-protein (GFP)-vinculin transfected 3T3 fibroblasts, and mouse macrophages were used. Gel-based tissue models were prepared by mixing cell suspensions with thawed Matrigel solution (BD Bioscience, Bedford, MA) using 1:1 proportion, and then solidifying it in the 37 °C incubator. Other components such as collagen I (BD Bioscience, Bedford, MA) were added to the gel with appropriate weight proportions to study the effects of matrix components on the OCT images. Cell and tissue cultures were maintained in an incubator at 37 °C and with 5% CO_2. For real-time imaging over extended time periods (days), tissue cultures were maintained in a portable microincubator (LU-CPC, Harvard Apparatus, Holliston, MA) that was placed on the microscope stages.

2.2 Cell migration assay

Matrigel-based invasion assays are a representative method of *in vivo* events. Porous filters were coated with a 3 mm-thick Matrigel layer and placed in a custom-made two-chamber system, modified from the Boyden migration chamber design [20]. Macrophage chemo-attractant, 100 nM of monocyte chemo-attractant protein-1 (MCP-1, Research Diagnostics Inc, NJ), was placed in the lower chamber and macrophages and Matrigel were placed in the upper chamber. Before beginning the migration assay, macrophages were starved in serum-free media for ~12 hrs. Then, the cell suspension containing $1x10^5$ cells was mixed with Matrigel to form a layer in the top chamber. The migration chamber was incubated in a humidified 5% CO_2, 37 ºC incubator for 2-3 hrs, before transferring to a microincubator for dynamic imaging under the OCT microscope. To validate cell migration, laser-scanning confocal microscopy was also used to image the 3-D tissue models. The cells were stained with CellTracker CMTMR (Invitrogen Corp., Carlsbad, CA) before being mixed with gel. Time-lapse confocal image z-stacks were obtained every 3 minutes.

2.3 Cell proliferation assay

Tissue models made of 3T3 fibroblasts and Matrigel were used in the cell proliferation assay. The tissue models were cultured in an incubator, and periodically removed for OCT imaging. OCT images were used to estimate the cell number increase in 3-D tissues. Similar samples were used for histological analysis. Frozen sections were stained with hematoxylin-eosin (H&E) for white-light histological observations.

2.4 Cell de-adhesion assay

The tissue model was made by seeding $5x10^4$ 3T3 fibroblasts in a 3-D calcium phosphate scaffold (BD Bioscience, Bedford, MA). After culturing for 3 or 10 days to achieve a low or high cell density, respectively, the tissue was immersed in the solution of 0.25% trypsin/EDTA. The tissue model was immediately and continuously visualized with OCT to track the dynamic process of cell de-adhesion from the scaffold.

2.5 Microstructured substrates

GFP-vinculin transfected fibroblasts cultured on flexible poly-dimethyl-siloxane (PDMS) microtextured (microgrooved) substrates with 3-D topographic features were employed to demonstrate the capability of OCT to visualize cell responses to substrate microtopographic features and examine cell-substrate interactions.

2.6 Optical coherence tomography

OCT imaging was performed on tissue models. Our fiber-based OCT system used a Nd:YVO_4-pumped titanium:sapphire laser as a broad-bandwidth optical source that produced

#71557 - $15.00 USD Received 31 May 2006; revised 19 July 2006; accepted 20 July 2006

300 mW of average power with an 80 MHz repetition rate at an 800 nm center wavelength. Laser output was coupled into an ultrahigh-numerical-aperture fiber (UHNA4, Thorlabs, Inc.) to spectrally broaden the light from 20 nm to more than 100 nm, generating the axial resolution of our system at 3 μm [21]. The reference arm of the OCT interferometer consisted of a galvanometer-driven retroreflector delay line that was scanned a distance of 2 mm at a rate of 20 Hz. The sample arm beam was focused approximately 1 mm deep into the tissue using a 12.5 mm diameter, 20 mm focal length achromatic lens. The 12 mW beam was scanned over the engineered tissue using galvanometer-controlled mirrors. The envelope of the interference signal was digitized to 12-bit accuracy. The transverse resolution was estimated to be 10 μm, which was the full-width at half-maximum of an isolated sub-resolution scatterer. Consequently, the imaging depth of 2 mm covered several Rayleigh ranges of the focused beam, and thus some loss of resolution was observed near the top and bottom edges of the images. For the applications described here, this choice of imaging lens provided an appropriate balance between resolution and depth-of-focus. However, recent advances in image formation for OCT are expected to provide depth-independent resolutions in future work [22].

2.7 Three-dimensional data reconstruction

Three-dimensional images were acquired over 10 minutes and reconstructed with SliceDicer (Pixotec, Renton, WA) or Amira (Image System, Minnetonka, MN).

3. Results and discussion

3.1 Cell migration

The Boyden chamber assay using microporous membrane inserts is the most widely accepted assay for cell migration and invasion [20]. In order to facilitate the dynamic imaging of cells, we fabricated a modified Boyden chamber system for a real-time cell migration assay in 3-D matrices and made it adaptable to a microincubator for long-term cell imaging studies (Fig. 1).

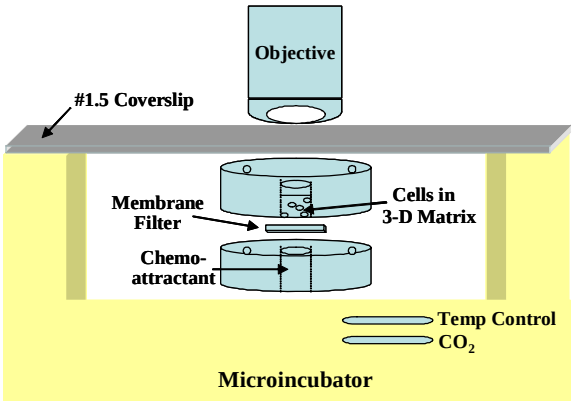

Fig. 1. Experimental set-up for cell chemotaxis migration studies. A modified Boyden chamber is shown, in expanded view to show the membrane filter, and contained with a microincubator chamber for long-term imaging studies on a microscope stage.

The microincubator was placed under an OCT microscope during the entire experimental period, providing cells optimal physiological conditions while migrating. The cells migrated towards the chemo-attractant, MCP-1, and migration parameters were measured with this chemotaxis assay. Figure 2 demonstrates the 3-D positional changes of the cells in the tissue model over time. Cell positions at each specific time-point were labeled with a specific color. Cell migration direction and velocity could be readily obtained from these OCT images. The migration speed in our experiment was approximately 0.67 μm/min (20 μm per 30 min), which correlated with that reported in the literature [23,24]. The migration speed was uniform throughout the 2 mm detection depth. By combining the time-lapse 3-D images into

#71557 - $15.00 USD Received 31 May 2006; revised 19 July 2006; accepted 20 July 2006

composite images (Figs. 2(g) and 2(h)), it was possible to track the paths traveled by individual cells and determine the distribution of phenomenological parameters, including cell speed. The cell migration speed decreased after 2 hours, but the cell density in the gel had increased, which may have been a contributing factor.

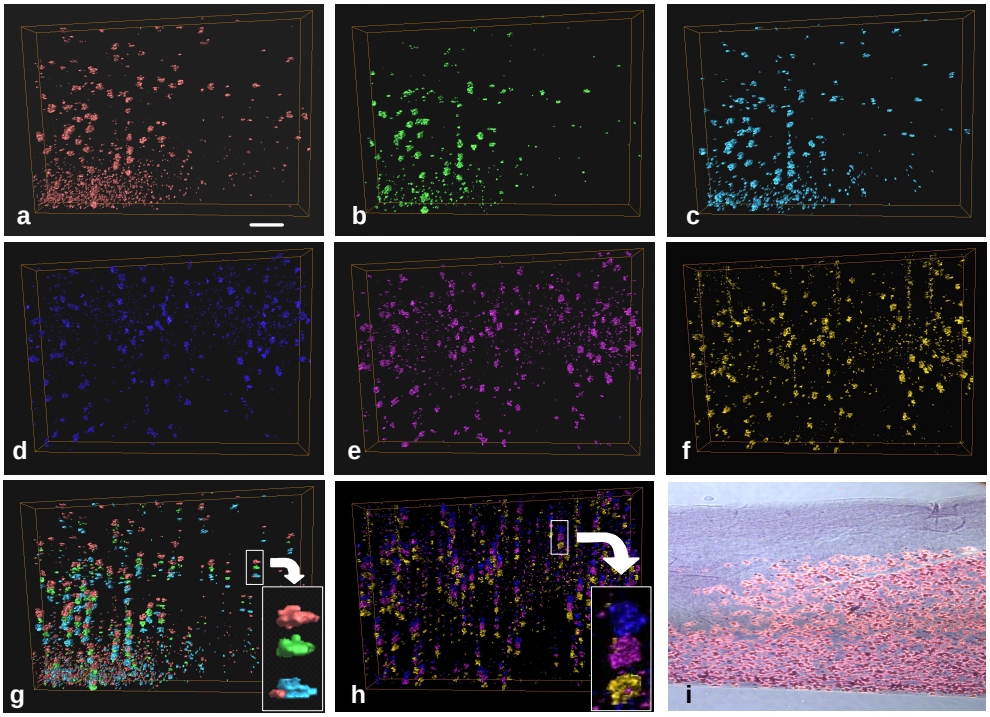

Fig. 2. OCT of cell migration. 3-D OCT images demonstrate the migration of macrophages (a-f). Cells at different points in time are labeled with different colors. The interval time is 40 min between (a/b, b/c, d/e, and e/f), and 120 min between (c/d). Individual OCT images are merged to form composite images of individual cell migration in 3-D space (g,h). Composite (g) is composed of (a-c) and composite (h) is a composed of (d-f). Insets in (g,h) show color-coded single-cell migration. Corresponding histology after the study is shown in (i), with macrophages collecting at the bottom. Scale bar is 200 µm.

Laser-scanning confocal microscopy was used to image cell migration with a similar setup. However, the imaging configuration of the confocal microscope was inverted, so the entire migration chamber system shown in Fig. 1 was subsequently inverted on the stage, which subsequently resulted in an upward trend in migration (Fig. 3). Compared to the OCT images, confocal images have higher spatiotemporal resolution. The migration speed observed in the confocal imaging studies was similar to that from OCT time-lapse images. Compared to the OCT imaging technique presented here, current methods of analysis of cell migration and invasion are time-consuming and tedious, involving cotton swabbing of non-migrated cells on the top side of the insert, manual staining, and counting. We present an approach for determining the cell migration speed, direction, and path, and evaluating the effect of isotropic variations in the extracellular environment on the tissue cell motility. OCT imaging provides a wider field-of-view, deeper imaging penetration, and the potential for long-term investigations because no probes or dyes are required. Confocal microscopy, however, in conjunction with dependent expression of fluorescent probes, can provide additional insight into functional parameters.

#71557 - $15.00 USD Received 31 May 2006; revised 19 July 2006; accepted 20 July 2006

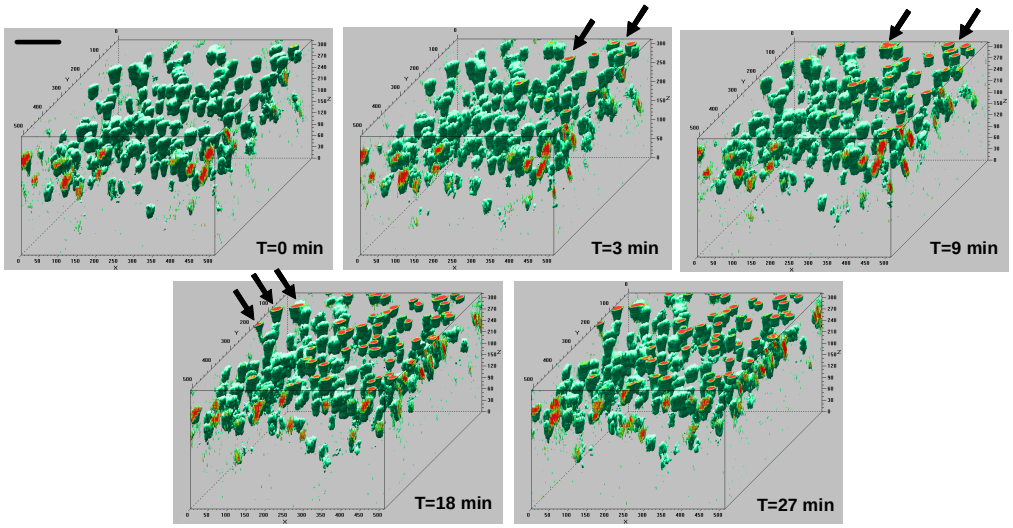

Fig. 3. Cell migration validation with confocal microscopy. 3-D confocal images of cell migration through the matrix is shown. Migration direction is upward as the microincubation chamber was inverted on an inverted microscope stage. Note the increasing number of cells entering the top plane of the volume (arrows) over time. Scale bar represents 50 µm.

Cell migration is an essential function of normal tissue processes, including embryonic development, angiogenesis, and wound healing. For example, the migration of precursor cells from the basal layer to the epidermis functions to continuously renew skin. Cell migration is also a fundamental process that can contribute to important pathologies. Leukocyte migration from the circulation into the surrounding tissue, where they ingest bacteria, is important for mounting an immune response. Chemotaxis assays usually are carried out to study the migration ability of cells in response to a chemical or biological factor. Much of our knowledge regarding migration has been obtained from cells growing on flat surfaces, such as coverslips or tissue culture dishes. Only recently have studies begun to examine migration in environments which more closely mimic that observed *in vivo*, such as 3-D matrices and tissue slice cultures. Migration modes and cell morphologies in 3-D environments can differ significantly from those observed with dissociated cells migrating on planar substrates [25]. Our approach has been through time-lapse 3-D OCT where the migration rates and directionality of cells in 3-D matrices can be readily measured.

This migration assay based on non-invasive optical imaging with OCT provides a rapid and efficient system for quantitative determination of factors on cell migration. Furthermore, chemo-attractants are potential therapeutic targets for intervention in wound healing, cancer, and inflammation. Our results suggest that it is possible to use OCT to evaluate the performance of various chemo-attractants.

3.2 Cell proliferation

Figure 4 illustrates representative OCT images used to track cell proliferation in 3-D tissue models. Both 2-D x-z images and 3-D reconstructed volumes are shown to demonstrate the cell proliferation. Compared to the cells cultured on a monolayer, cells seeded in a 3-D matrix might encounter matrix resistance to migration. Thus, cells divide and form aggregates at the original sites in the matrix. After days of proliferation, the tissue model is comprised of cell aggregates and exhibits a more heterogeneous cell distribution. Therefore, the cell number increase is demonstrated by the increasing size of the cell aggregates in 3-D OCT images.

Due to the limits of the OCT axial and transversal resolution (3 µm and 10 µm, respectively), small gaps among the cells cannot be observed. Thus, single cells in close proximity cannot be resolved. As a result of proliferation, growing clusters or aggregates of

#71557 - $15.00 USD Received 31 May 2006; revised 19 July 2006; accepted 20 July 2006

cells were seen in the images. Nevertheless, the cell proliferation rate may still be quantified by the diameter of the cell aggregate assuming that the gaps among the cells are much smaller than the cell diameters. Because of the 3-D structure, changes in the scattering volume, instead of the scattering area, should be used in the proliferation measurement. In this case, we estimated the proliferation rate in the tissue model with low initial cell density from Day 0 to Day 3 was 4 times, and that from Day 3 to Day 6 was 4 times as well. The results were confirmed using the histological analysis. This proliferation rate is typical for cells within engineered tissue scaffolds, but is highly dependent on the cell type, microenvironment, and culture conditions.

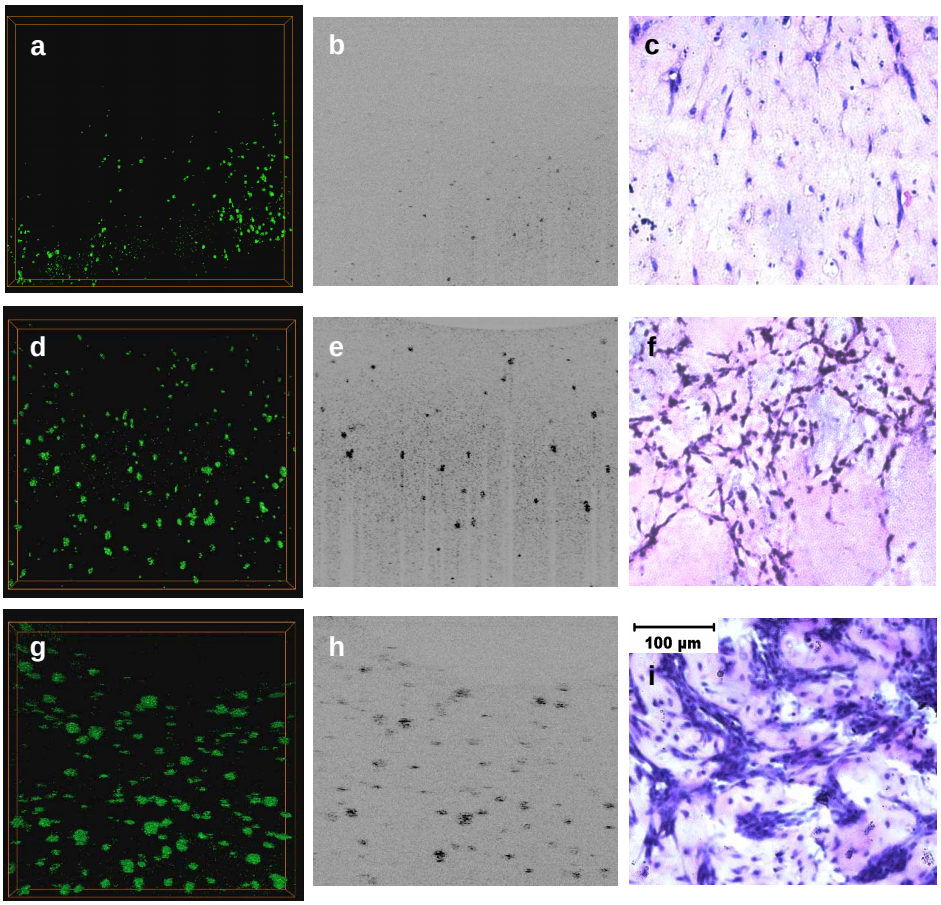

Fig. 4. OCT of cell proliferation in 3-D scaffolds. Images were acquired with low ($5x10^4$ cells) initial cell density. 3-D OCT images (a,d,g) and 2-D (x-z) OCT images (b,e,h) of engineered tissues were acquired on Day 0 (a-c), Day 4 (d-f), and Day 8 (g-i). Histological images stained with H&E (c,f,i) are shown to confirm cell proliferation over time. Scale bar in (i) is applicable for all images.

Cell proliferation provides tissue engineering researchers with the comprehensive level of information on biochemical environments for cell growth. In addition, cell proliferation is an important measurement in cell-based screening for efficiency of therapeutic drugs (e.g. drugs for cancer). Histological assays only provide end-point information. The OCT imaging approach can provide a real-time, straightforward, and accurate estimation of cell number and proliferation rate in 3-D tissue models.

#71557 - $15.00 USD Received 31 May 2006; revised 19 July 2006; accepted 20 July 2006

3.3 Cell de-adhesion

For cell de-adhesion assays, tissue models were incubated with 0.25% trypsin/EDTA at room temperature. Figure 5 shows the process of cells detaching from a calcium-phosphate scaffold. Time-lapse images demonstrate different de-adhesion processes in an engineered tissue under short-term culture (3 days, Fig. 5(a)) from that under long-term culture (10 days, Fig 5(b)). The tissue model under short-term culture has a low density of cells and secreted matrix. The images shown were taken after 10 min, with little change noted in the images before 10 min. De-adhesion of cells could be observed based on the optical scattering changes in the OCT images (Fig. 5(a)). As shown in the cell proliferation data, when cells are close to each other, tightly packed, and adhered, our OCT system was not able to resolve individual cells nor differentiate cells from the scaffold. Thus, images in this time-lapse series appear nearly structurally identical except for the difference in the scattering contrast (Fig. 5(a)). Comparing images at different points of time, the loss of optical scattering, which implies the loss of cells on the scaffold, could be assessed. The tissue exhibited a gradual decline in the optical scattering between 10 min and 16 min, which suggests that cells de-adhered from the scaffold slowly over this time. Difference images were used to illustrate these scattering changes, which were repeatable, and controlled for specimen positioning, fluctuations in laser power, and media evaporation.

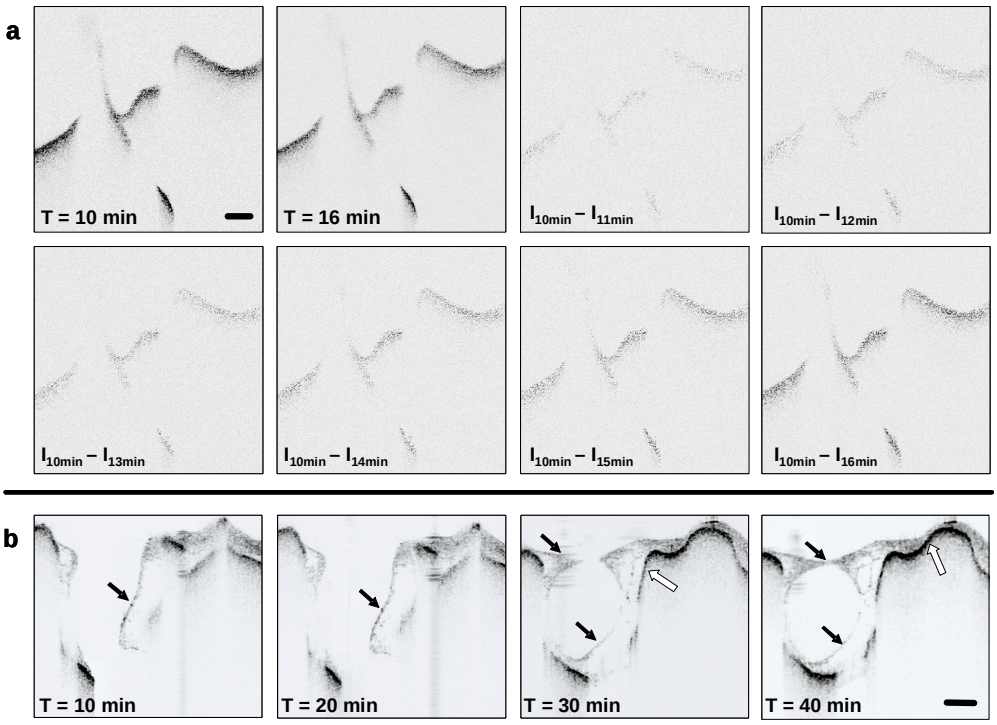

Fig. 5. OCT of cell de-adhesion. Time-lapse images showing the process of cell de-adhesion and cell layer movement (black arrows) from a calcium-phosphate scaffold. Cells were cultured on the scaffolds for (a) 3 days and (b) 10 days. Continuous images were taken every minute after engineered tissues were soaked in a trypsin solution. (a) OCT images acquired at 10 min and 16 min after placement in trypsin solution. No detectable change was noted before 10 min. Difference images were calculated during cell de-adhesion by subtracting images acquired at later time-points. (b) Time-lapse images showing the process of cell layer de-adhesion (black arrows) from the scaffold (white arrows). De-adhesion of the cell-layer sheet was abrupt between 20 min and 30 min. Scale bars represents 200 µm.

#71557 - $15.00 USD Received 31 May 2006; revised 19 July 2006; accepted 20 July 2006

In contrast, the de-adhesion process in the tissue model which was cultured for 10 days with a very high density of cells and secreted matrix showed abrupt changes in the OCT image (Fig. 5(b)) instead of gradual scattering changes. In response to the trypsin-EDTA, it was observed that entire layers of cells were de-adhered from the 3-D scaffold. For tissue models with high cell density, it is apparent that cells had formed multiple layers on the scaffold. Dynamic OCT imaging of the model demonstrates the dynamic de-adhesion process of the cell layers off of the scaffold. Because thick layers of numerous cells moved off the scaffold at one time point, the cell-scaffold images look different before and after the de-adhesion process. After de-adhesion, the scaffold (shown with white arrows), which could not be distinguished from the cells previously, could be identified. A similar observation is well known in flask-cultured cells. Flask-cultured fibroblasts with a short culture time detach from the flask surface individually by trypsin-EDTA. After trypsinization, floating, isolated cells are observed. With the increase of culture time, because of matrix deposition, cells become more and more difficult to detach, and more and larger cell aggregates are observed. Flask-cultured fibroblasts with long-term culture eventually form an intact cell-matrix sheet and detach from the surface together in a layer. It has been shown that the fibroblasts and many other cell types are capable of depositing extracellular matrices on the substrate or the 3-D scaffold, thus forming cellular sheets over time [26-28]. Because the cells in the sheets are strongly connected by matrices, it is difficult to use trypsin-EDTA to separate them. Trypsin breaks the cell-scaffold adhesion, but not the cell-matrix adhesion. As a result, a complete cellular sheet of cells, instead of individual cells, detatch from the scaffold simultaneously.

Cell adhesion and de-adhesion are fundamental processes that are critically involved in embryonic development and many diseases. One of the most important properties of cells that are derived from multicellular organisms is their ability to adhere to and migrate through extracellular matrices and 3-D structures. OCT has the potential for following these dynamic processes in the developing engineered tissue model, particularly where artificial scaffolds play a central role for defining the early morphology of the tissue.

3.4 Cell-material interactions

Cells seeded on microtextured substrates were used to examine the cell-material (structure) interactions (Figs. 6 and 7). Two types of microtextured substrates were used in the studies. One type (Fig. 6) was characterized by an array of parallel microgrooves with dimensions of 30 μm x 30 μm x 40 μm (width x height x spacing), and the other (Fig. 7) was characterized by an array of microgrooves with dimensions of 10 μm x 10 μm (width x height) and spacing varying from 5 μm to 20 μm. Compared to phase-contrast microscopy, OCT can reveal the 3-D substrate microstructures as well as the interactions between the cells and the microstructure in topographic substrates in 2-D and in 3-D.

OCT images also demonstrate differences in cell-material interactions due to the topographical microstructures. On the microgrooved microstructures with features larger than the size of single cells (Fig. 6), the cells have visualized adhesions on and within the microgrooved structures (Figs. 6(d-f)). In the OCT images, the cells spread and extended to the bottom of the microstructure (as shown with black arrows in Fig. 6), and thus represent active interactions with the structure. This result can be confirmed using confocal microscopy to image the GFP-labeled vinculin (cell focal adhesion sites) in these transfected cells (Figs. 6(h) and 6(i)). Compared to the 3-D confocal image (Fig. 6(i)), OCT images can show 3-D microgroove structures and delineate the cell-structure interactions (Fig. 6(f)).

On microgrooved microstructures with features smaller than the size of single cells (Fig. 7), the cells form large clusters on top of the grooved microtopography (Figs. 7(b) and 7(c)) and do not have active interactions with the structure. This might also be due to the hydrophobic nature of the silicone substrate. Hydrophobic surfaces prevent cell adhesion because they are unfavorable for the attachment of adhesive proteins. Therefore, cell-cell adhesion may cause the cells to preferentially form a larger cluster if the initial cell-substrate adhesion is weak. On the microgrooved substrate with features larger than single cells, individual cells or small cell clusters can attach to and within the microgrooved substrate in a

#71557 - $15.00 USD Received 31 May 2006; revised 19 July 2006; accepted 20 July 2006

similar way as to a flat surface because the substrate structure is proportionally larger than the cells. On the microgrooved substrate with features smaller than single cells, the initial cellular attachment is more difficult because of the substrate topography, which may cause the cells to aggregate before attaching to the substrate. Therefore, the cellular clusters grow on top of the microgrooved topography instead of interacting with the 3-D structure.

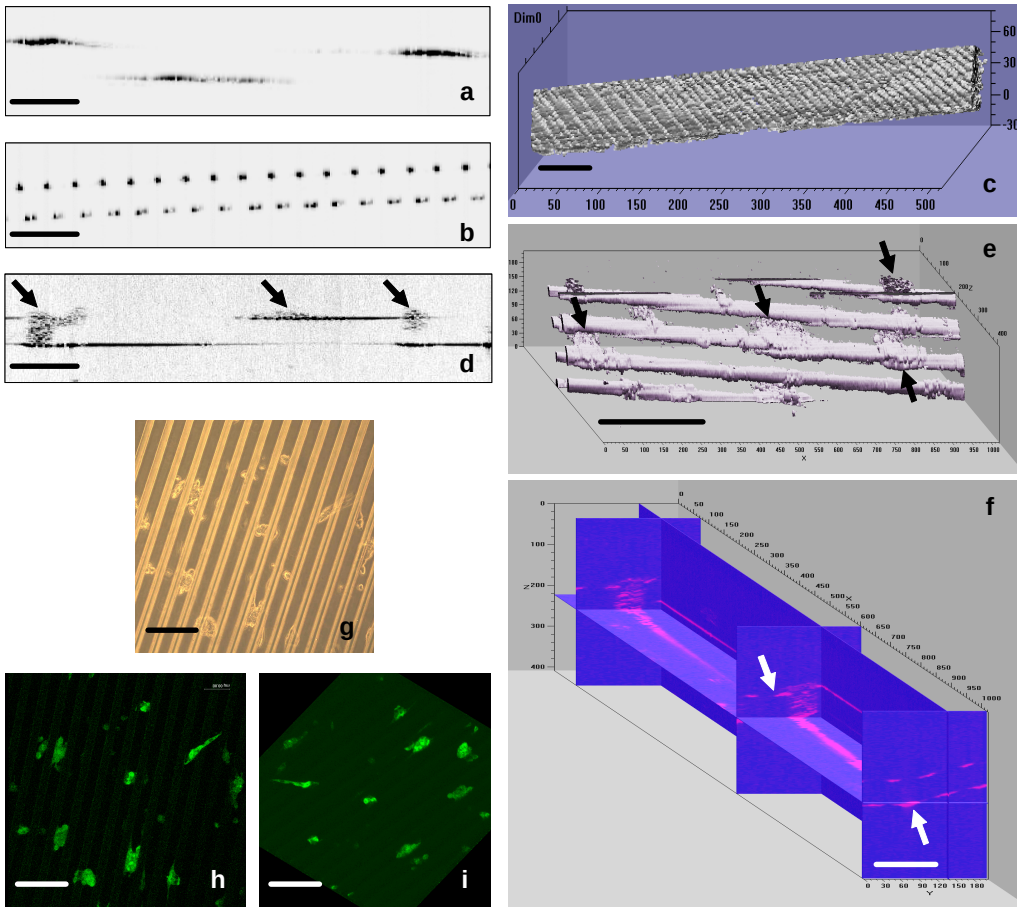

Fig. 6. OCT imaging of cell-substrate interactions with microtopographic feature sizes larger than single cells. 2-D (a,b) and 3-D (c) OCT images of a microgrooved (30 µm x 30 µm x 40 µm) PDMS substrate used for cell culture (d-f). Black arrows show the cells interacting with the substrate microstructure. OCT images are compared with corresponding phase contrast (g), 2-D confocal microscopy (h), and 3-D confocal microscopy (i) images. White arrows show the cross-sectional structure of the microgrooves. Scale bar represents 100 µm in all images.

#71557 - $15.00 USD
Received 31 May 2006; revised 19 July 2006; accepted 20 July 2006

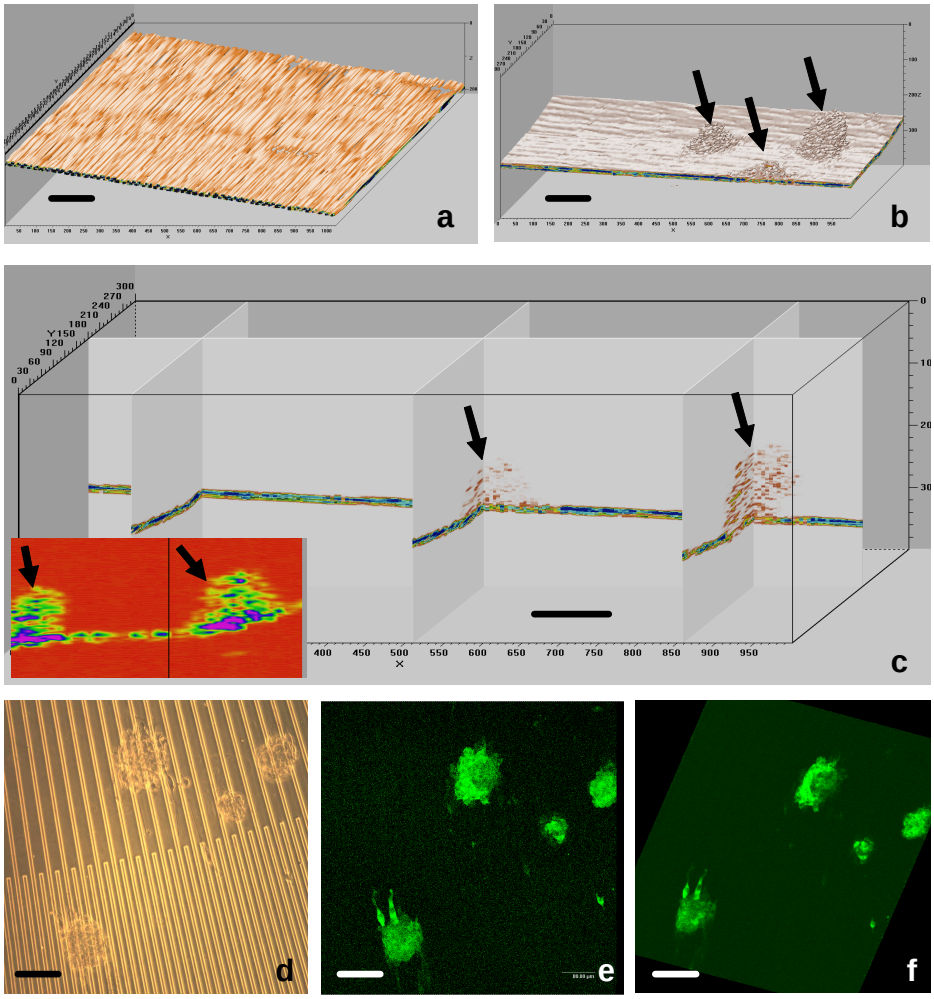

Fig. 7. OCT imaging of cell-substrate interactions with microtopographic feature sizes smaller than single cells. 3-D OCT images of a microgrooved (10 µm x 10 µm x 5-20 µm) PDMS substrate without (a) and with (b,c) cultured cells. Black arrows indicate cell clusters. Inset in (c) illustrates cell clusters overlying microgrooves. OCT images are compared with corresponding phase contrast (d), 2-D confocal microscopy (e), and 3-D confocal microscopy (f) images. Scale bar represents 50 µm in all images.

3.5 Matrix influencing effects

During these investigations, we found that the scaffold matrix composition significantly influences the signal content within OCT images (Fig. 8), which is relevant to other investigators wishing to pursue cell-imaging studies with OCT. The addition of collagen I reduces the visibility of cells in the 3-D matrix. This may be caused by the scattering effects specific to the collagen, which may have similar optical scattering properties as the cells. This suggests a potential limitation of OCT systems for the real-time imaging of cell activities in 3-D tissue models over time. Scaffold matrix materials must be selected to have different scattering properties from the cells and from the extracellular matrix that is gradually secreted by proliferating cells over time. Ongoing studies are investigating the most appropriate scaffold matrix materials and composition to optimize OCT signal differentiation between

#71557 - $15.00 USD Received 31 May 2006; revised 19 July 2006; accepted 20 July 2006

cells and scaffold during the physiological-dependent and microenvironmental-dependent changes that occur during the development of engineered tissues.

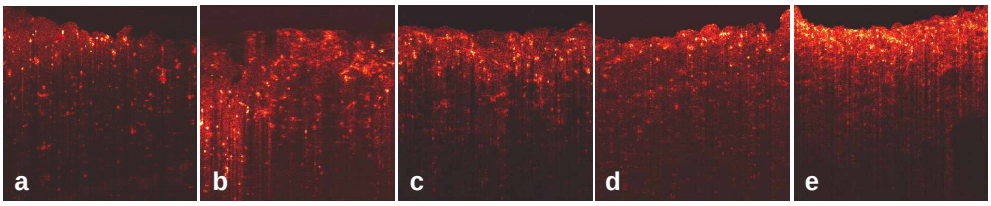

Fig. 8. Collagen-dependent changes in OCT. OCT images of tissue models are shown with a constant cell number (~ 5 x 10^4) and increasing amounts of collagen in the Matrigel matrix. Collagen percentage varies for (a) 0%, (b) 0.05%, (c) 0.1%, (d) 0.15%, and (e) 0.2%. Increasing collagen content increases scattering, reducing imaging depth and contrast between cells and matrix. Scale bar represents 100 μm.

4. Conclusion

Visualizing the 3-D organization and dynamics of cells in relation to their surrounding biochemical and biomechanical environments in an unperturbed or perturbed context requires a noninvasive, high-resolution, imaging technique. In this paper, we described our approach which uses a four-dimensional (3-D space over time) high-resolution OCT system in conjunction with 3-D cell and tissue culture and assay techniques. We demonstrate that OCT, frequently used for generating histology-like images of tissue structure, can also be used to track and analyze cell dynamics in tissue models.

Three-dimensional cell-based tissue models have become increasingly useful in the fields of tissue engineering, drug discovery, and cell biology. While techniques for building these tissue models have advanced, there has been an increasing demand for imaging techniques that are capable of assessing complex 3-D cell behaviors in real-time, and at the depths that comprise thick tissues. Understanding these cell behaviors requires advanced imaging tools to progress from characterizing 2-D cell cultures to more complex, highly-scattering, thick 3-D tissue constructs. OCT is an emerging biomedical imaging technique that can perform cellular-resolution imaging in living and developing tissue models in real-time. We have demonstrated that it is possible to use OCT to evaluate dynamic cell behavior and function in a quantitative fashion in four dimensions (3-D space over time). This powerful approach to the noninvasive imaging of the morphology and function of tissue models has enormous potential for a wide range of applications ranging from tissue engineering to drug discovery.

Acknowledgments

We wish to thank Dr. Daniel Marks of the Beckman Institute for Advanced Science and Technology for his technical contributions to the image acquisition software and for his intellectual contributions to the design of this imaging system. This work was supported in part by the National Institutes Health (NIBIB, 1 R01 EB00108, S.A.B.), and the University of Illinois Critical Research Initiative (S.A.B.). Dr. Wei Tan is currently at the University of Colorado at Boulder, Department of Mechanical Engineering. Dr. Tejal Desai is currently at the University of California – San Francisco, Departments of Physiology and Bioengineering. Additional information can be found at http://biophotonics.uiuc.edu.

#71557 - $15.00 USD Received 31 May 2006; revised 19 July 2006; accepted 20 July 2006